



OPEN Development of rare earth element-based hybrid aluminium composites using stir casting process

Gaurav Sapkota¹, Ranjan Kumar Ghadai²✉, Soham Das¹, Asish Sharma³, G Shanmugasundar⁴, Robert Čep⁵ & Kanak Kalita^{6,7}✉

Aerospace and marine industries are constantly in search of materials that can provide good strength and durability while also being lightweight. Aluminium composites with adequate reinforcements have been proven to be effective in achieving incredible mechanical properties while also maintaining a good strength to weight ratio. Numerous studies have been done to study the various possibilities of matrix reinforcement combinations in aluminium composites. This work focuses on studying the effect of varying Cerium Oxide (CeO₂) percentage in the aluminium composite on its tensile strength, hardness and corrosion resistance. CeO₂ is used along with Silicon Carbide (SiC) and Multi-Walled Carbon Nanotubes (MWCNT) to develop four samples of hybrid aluminium composites with SiC and MWCNT constituting 1% and 0.1% of the composite and the weight percentage of CeO₂ is varied between 1 and 2.5%. All the samples were fabricated using the modified stir casting process. The results show that the hardness and tensile strength of the composites peak when the CeO₂ is at 2% while corrosion resistance only gets better with increasing reinforcement content. A significant enhancement in mechanical and physical properties of aluminium composite suggests that MWCNT is an effective hybridizing agent with SiC and CeO₂ to develop aluminium composites.

The progress of civilization has historically been guided by the ability of humanity to optimally utilize the material resources at their disposal¹. The significance of materials becomes evident when one observes the named eras in history, such as the Stone Age, Copper Age, Bronze Age, and Iron Age, each denoting the predominant materials used during various historical periods. With the rapid growth of technology since the 1830s, the importance of improved materials that would meet industrial requirements has been continually increasing². This demand has driven the development of materials that possess qualities like strength, hardness, and lightness, tailored to cater to the needs of industries in aerospace and automotive sector³.

Composite materials have gained a lot of traction among researchers and in industries due to the scope of applications that have surfaced in the past few decades⁴⁻⁷. These materials have become highly preferred due to their potential to be customized and designed with specific properties^{8,9}. The automotive industries can benefit enormously from materials that have a good strength-to-weight ratio^{10,11}. Composites are developed by incorporating reinforcements into matrix material wherein matrix materials act like binders that distribute load among reinforcements which are the load bearing members in the composite¹². This leads to a general strengthening of the materials while also retaining the ductility of the matrix materials¹³. Aluminum alloys offer an excellent combination of strength with low density and, therefore, a good choice of matrix material for the development of composites. The application of aluminum alloys has grown in recent decades to cater to a wide range of industries including shipbuilding, the automobile, and heavy machinery industry^{14,15}. Conventionally, the choice of reinforcements was limited to ceramic particles because the goal was primarily strengthening¹⁶⁻¹⁸. Baraily et al.¹⁹ developed Silicon Carbide (SiC) and flyash bagasse ash reinforced composite with enhanced

¹Department of Mechanical Engineering, Sikkim Manipal Institute of Technology, Sikkim Manipal University, Gangtok, India. ²Department of Mechanical and Industrial Engineering, Manipal Institute of Technology, Manipal Academy of Higher Education, Manipal, Karnataka 576104, India. ³Khangchendzonga State University, Sikkim, India. ⁴Department of Mechanical Engineering, Sri Sairam Institute of Technology, Chennai 600044, India. ⁵Department of Machining, Assembly and Engineering Metrology, Faculty of Mechanical Engineering, VSB-Technical University of Ostrava, 70800 Ostrava, Czech Republic. ⁶Department of Mechanical Engineering, Vel Tech Rangarajan Dr. Sagunthala R&D Institute of Science and Technology, Avadi 600 062, India. ⁷Jadara University Research Center, Jadara University, Jadara, Jordan. ✉email: ranjankumarbls@gmail.com; drkanakkalita@veltech.edu.in

Mg	Si	Fe	Cu	Mn	Cr	Zn	Ti	Others	Al
0.45–0.9	0.2–0.6	0.35	<0.1	< 0.1	0.1	<0.1	< 0.1	0.15	Max

Table 1. Chemical Composition of AL-6063 in terms of weight percentages of constituent elements.

Sample designation	Matrix material	SiC (%)	MWCNT (%)	CeO ₂ (%)
Sample 1	Al-6063	1	0.10	1
Sample 2	Al-6063	1	0.10	1.50
Sample 3	Al-6063	1	0.10	2
Sample 4	Al-6063	1	0.10	2.50

Table 2. Sample designations and composition.

corrosion properties. Bhowmik et al.²⁰ developed a hybrid aluminium composite using SiC and titanium bromide powders as reinforcements using stir casting route. The developed composite showed enhanced hardness and tensile strength. Similar literature are available that reflects the effect of ceramic reinforcements on mechanical and tribological properties. However, with the advancements in research on material science and engineering, reinforcements have much more to offer in addition to strengthening²¹. Pazhani et al.²² developed graphene-reinforced aluminium composites using a novel squeeze-casting technique for lightweight aeronautical applications. The developed composite had an increased tensile strength and enhanced hardness making it a more robust material for aerospace applications. Akinwande et al.²³ in their recent work used a commercially available high entropy alloy as reinforcement to develop an aluminium composite using powder metallurgy route. Besides the obvious strengthening of the composite, it also showed enhanced tribological properties. Ananiadis et al.²⁴ also used high entropy alloy particles to reinforce aluminium composites and their work revealed that a significant enhancement in corrosion properties was observed in the developed composite. Samal et al. used B₄C and Multi Walled Carbon Nanotubes (MWCNT) to develop aluminium composite using A383 as the matrix material. The developed composite showed enhanced micro-hardness and tribological properties. Although MWCNT bears exceptional potential as a new age reinforcing material because of its excellent mechanical properties, it is less studied upon as a reinforcement with aluminium composite. Literatures that are available on MWCNT as reinforcement show promising results that serves as a basis for the current work to consider MWCNT as one of the reinforcing material.

Among the newly found reinforcement materials are the rare earth element-based compounds that have gained huge popularity among researchers in recent years. They are primarily used as a hybridizing agent that adds so much to the properties of composites by incorporating them in trace amounts. Cheneke and Karunakar²⁵ published a work on the incorporation of yttria with titanium boride to develop a composite using the rheocasting technique. Yttria incorporated composite had at least an additional 20% increase in all the mechanical properties studied in comparison with the titanium boride-reinforced composite. Kumar et al.²⁶ used a powder metallurgy route to develop CeO₂-reinforced composites by varying CeO₂ weight percentages. The study suggests that the reinforcement effectively enhances the corrosion resistance properties of aluminium alloy besides the obvious increase in tensile strength and hardness. Kumar et al.²⁷ also suggest that cerium oxide (CeO₂)-reinforced composites also exhibit self-lubricating properties which add to the overall robustness of the material. Similar works on CeO₂, lanthanum oxide (La₂O₃) etc. are abundantly available to establish the utility of rare earth-based reinforcements.

Although rare earth element-based reinforcements have shown promising results with aluminum composites in the works that have been done so far, the literature that explores this possibility is very limited. Furthermore, the literature that explores this possibility is limited by the choice of reinforcement that explores only ceramic particle-based reinforcements with rare earths. It is evident from the literature that the options for reinforcement materials have opened up in aluminium composites, yet there seems to be a lack of literature that deals with a peculiar combination of reinforcement materials that includes a conventional reinforcement like SiC, a modern-day material like MWCNT and a suitable hybridizing agent in the form of rare earth based reinforcement like CeO₂. The current work is an attempt to bridge this gap by combining SiC, MWCNT and CeO₂ to develop a hybrid aluminium composite. The weight percentage of CeO₂ is varied while keeping the other two constant to develop four samples of aluminium composites using the stir casting method. These composites are characterized based on their morphological, mechanical and corrosion properties to assess the effect of CeO₂ on the studied properties.

Materials and methods

Development of composite

For the development of composite, Aluminium 6063 was chosen as the base alloy because of its widespread uses in making various aeroplane components. The chemical composition of the alloy is given in Table 1. The alloy was cut into small pieces and weighed 500 gms using a precision digital weighing machine. For reinforcements, SiC (particle size: 320 mesh), MWCNT (length: <10 μm dia: < 20 nm) and CeO₂ (APS: <50 μm) were used. The percentage composition used in each sample is presented in Table 2. Existing research work on the same

reinforcements was referred to choose a baseline weight percentage for each reinforcement, and numerous trial experiments were performed with varying weight percentages to arrive at the weight percentage for which the least agglomeration was observed in the available stir casting set-up. The stir casting set-up used for the development is shown in Fig. 1. A bottom-pouring setup facilitated a smooth passage of molten aluminum mixed with reinforcements for better particle distribution while also preventing the slag from passing through to solidify in the mold placed below^{28–31}. Aluminium pieces are heated in a steel crucible to reach the temperature of 730°C. A four-blade stirrer is used to create a vortex inside the melt by rotating it at 400 RPM. The reinforcements are heated at 280°C inside a muffle furnace before adding them into the vortex. The preheating of reinforcements is done to remove any moisture present in the reinforcement particles and improve the wettability with molten aluminium. The melting furnace is covered with a ceramic plate to isolate the molten aluminium with atmospheric oxygen to minimize oxidation of molten aluminium. The mixture was stirred for 7 minutes at 400 RPM before pouring it down to the steel mold preheated to 325°C. It should be mentioned here that the stirring process parameters were adapted from existing literature and modified to align with the operational conditions of the available setup based on numerous trial experiments. The preheating of mould is done to reduce the chances of defects that result out of trapped air and also to minimize the temperature gradient to facilitate a slow cooling rate. The solidified composite is then shaped appropriately following the various ASTM standards for microstructural, morphological and mechanical testing using various machining processes.

Characterization and testing

The developed as-cast composite taken out of the mold is shown in Fig. 2. Small cut-outs from various portions were prepared and polished to characterize the composite on their morphological and compositional properties. Scanning Electron Microscopy (SEM) and Electron Diffraction Spectroscopy (EDX) were done in CIF, Manipal, Udipi to study the microstructural properties of the composite. The images were taken at various magnifications to highlight various aspects of the microstructural properties of the composite. The composition of the composite was also validated using the X-ray diffraction (XRD) tests. Particles scattered from 0 degrees to 120 degrees were collected and the peaks were studied to study the composition of the composite.

To check for porosity in the as-cast sample, theoretical and experimental densities of the developed samples were compared to calculate a porosity index (PI) or void fraction (VF) using the formula shown in Eq. (1).

$$PI/VF = 1 - \frac{\text{Experimental density}}{\text{Theoretical Density}} \times 100 \quad (1)$$

Three different cutouts from various locations of the composite were used to estimate the experimental density using the Archimedean principle following the ASTM B962 standards using water as the immersion fluid. The theoretical density of the developed composites was calculated using the rules of mixtures. Relationship between density, weight and volume was used to calculate the volume percentages of all the reinforcements.

Electrochemical corrosion tests of all samples were done using standard Ag/AgCl as the reference electrode and Platinum as the counter electrode. 1M NaCl solution was used as the electrolyte for the test. Small samples measuring 3 mm × 3 mm × 25 mm were cut out from the composite which was used as the working electrode for the test. The applied potential was slowly ramped up from -1V to -0.5 V to obtain a Tafel plot for all the

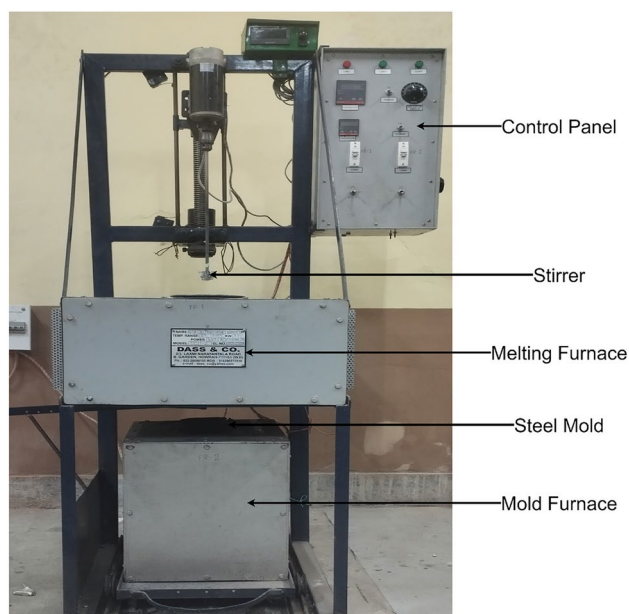


Fig. 1. Stir casting setup.

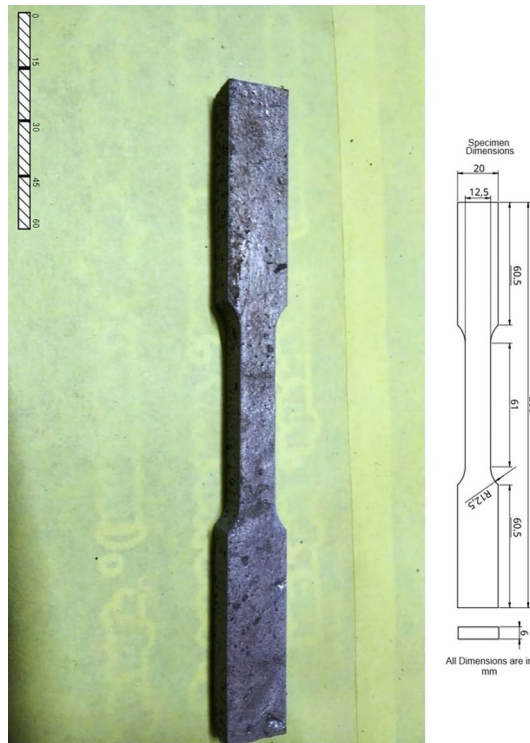


Fig. 2. Tensile test specimen as per ASTM E8 standards.

samples. Theoretical and Experimental densities of all the samples were also calculated using the rule of density of mixtures and Archimedes Principle respectively to calculate the porosity of the developed composite.

The hardness test samples were prepared by cutting out a few $10 \times 10 \times 4$ mm specimens from each sample and cleaning them with emery papers. Vickers hardness test was used to measure the hardness of the composite. Indentation was made at three different spots on each sample and the indentation diagonal was measured. The hardness value was calculated using the formula given in Eq. (2)

$$HV N = 1.854 \left(\frac{F}{D^2} \right) \quad (2)$$

and the average hardness was calculated by summing up hardness values for all observations for a given sample. This procedure was adopted to ensure the reproducibility of the results. The tensile test sample was performed according to ASTM E8 standards for sheets as shown in Fig. 2. Two samples each of the five samples, including an as-cast Al-6063, were machined according to the dimensions shown in Fig. 2 using wire EDM to shape the developed samples into the desired tensile test specimen. These Tensile test specimens were sent to the Kalinga Institute of Technology wherein the INSTRON Tensile Testing setup was used to measure the ultimate tensile strength.

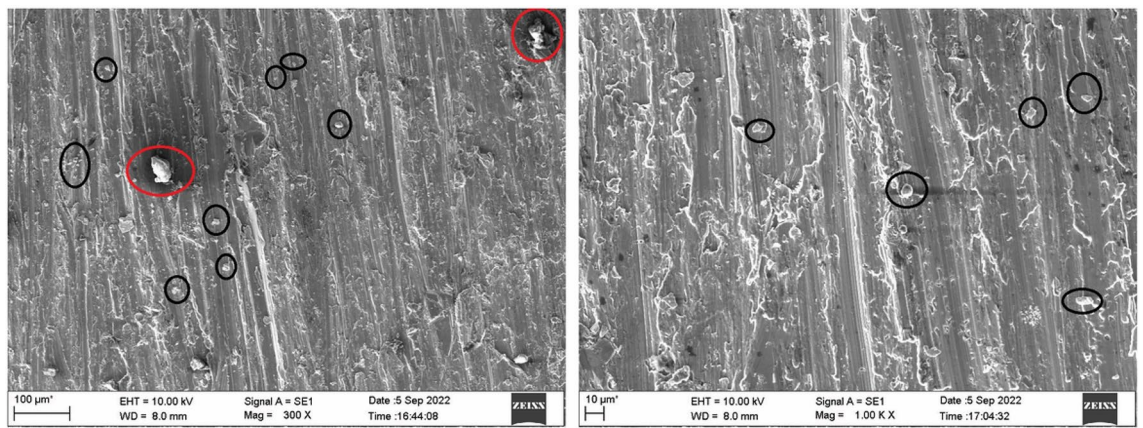
Results and discussion

Morphological and compositional characterization

SEM images for all 4 samples at various magnifications are shown in Figs. 3, 4, 5 and 6. The SEM images show elongated dendritic structures as a result of slow solidification because the sample was allowed to furnace cool in a controlled temperature setup. These images also reveal traces of particles present here and there (encircled in black). These may be SiC or CeO₂ particles incorporated as micro-sized powders. The distribution of SiC and CeO₂ can also be estimated using the colour mapping of carbon and cerium in the composite shown in Fig. 7.

Figures 3, 4, 5 and 6 suggest that they are scarcely present and distributed relatively homogeneously with intermittent traces of agglomeration visible throughout the sample which seems to be unavoidable. MWCNT, however, is visible when the magnification is increased to 1000x where small tubular particles are visible and dispersed through the matrix. These are also present in scarce quantity and slight agglomeration of these particles is visible which is shown in Figs. 3, 4, 5, 6 and 7 by encircling them in red. EDS peaks also elucidate the presence of CeO₂, SiC and SiO₂ in the aluminium matrix. SiO₂ is formed as a result of oxidation of SiC during preheating of reinforcements and is responsible for strengthening the matrix-reinforcement bond with SiC, which is a ceramic particle with very poor bond strength with metals like aluminium.

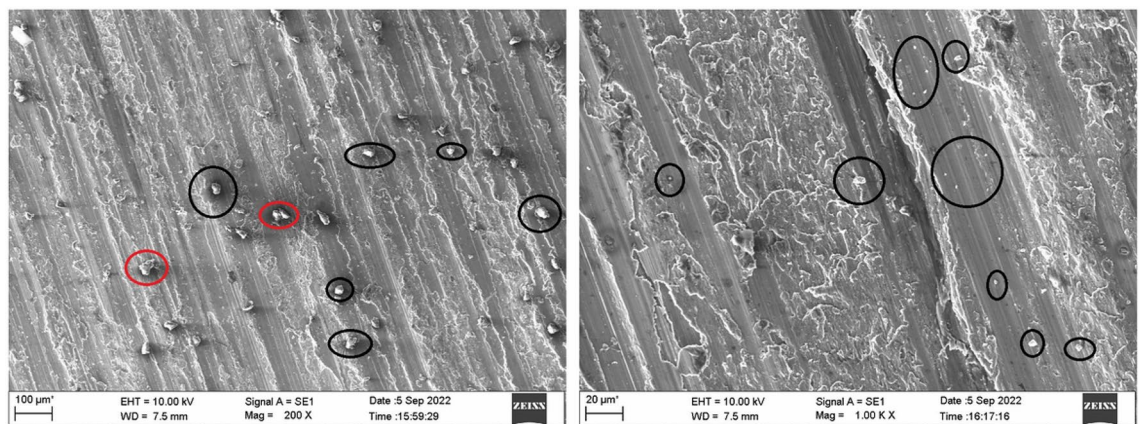
Figure 8 shows the XRD pattern of Al MMC developed using the stir casting process. The measured XRD peaks fall between 20° and 90° in the 2θ diffraction range. XRD results show prominent peaks within the range



(a)

(b)

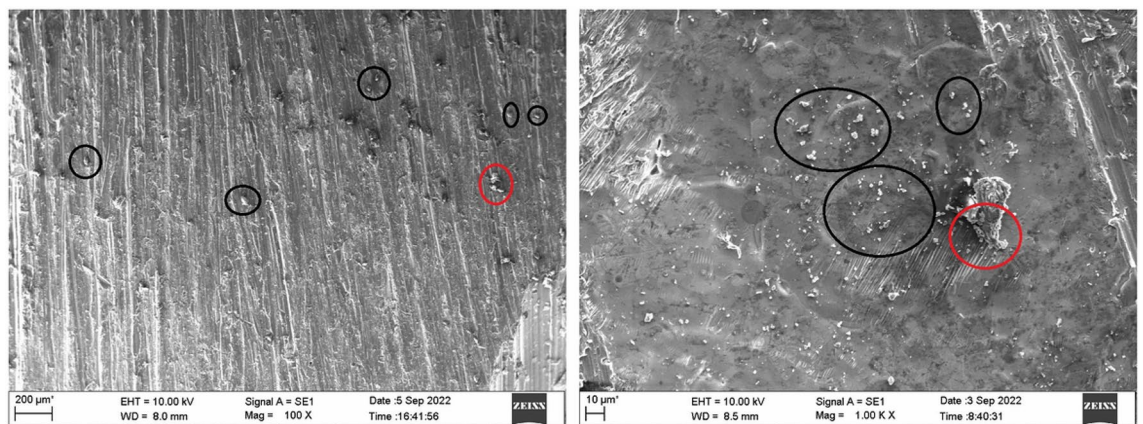
Fig. 3. SEM image of sample 1 at different magnifications (a) Low magnification (b) High Magnification.



(a)

(b)

Fig. 4. SEM image of sample 2 at different magnifications (a) Low magnification (b) High Magnification.



(a)

(b)

Fig. 5. SEM image of sample 3 at different magnifications (a) Low magnification (b) High Magnification.

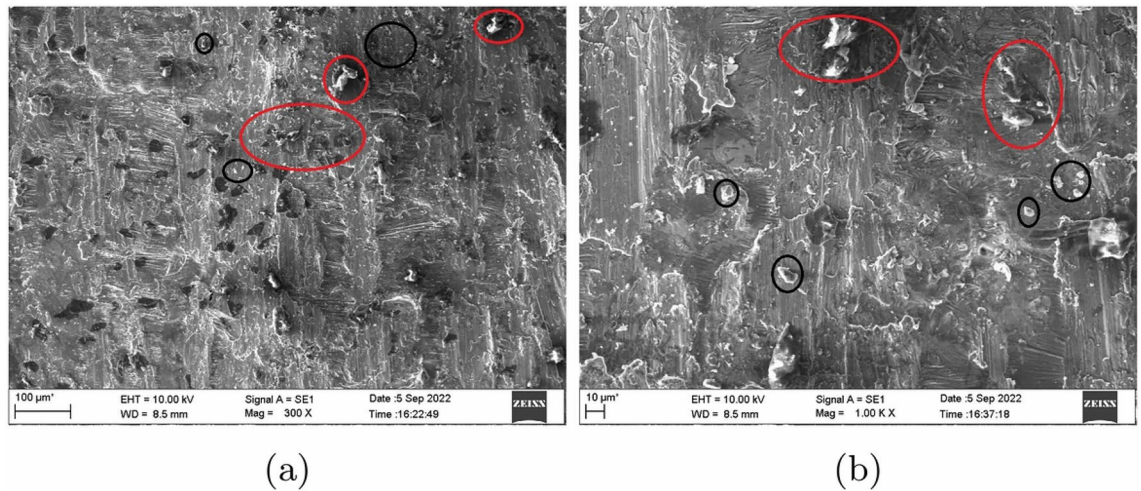


Fig. 6. SEM image of sample 3 at different magnifications (a) Low magnification (b) High Magnification.

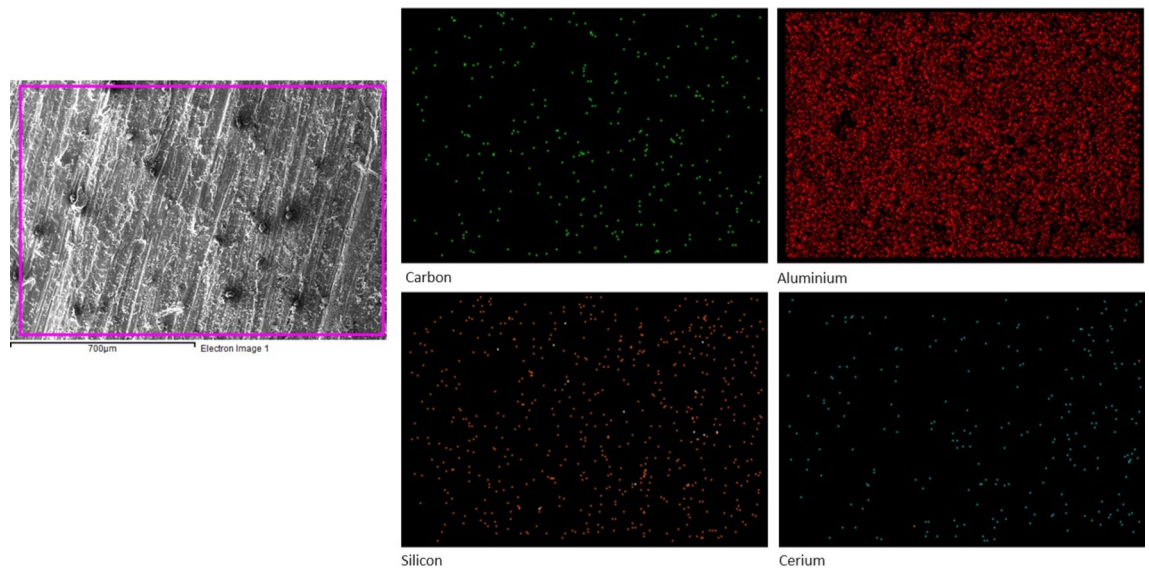


Fig. 7. Colour Mapped SEM Images for Sample 4 highlighting the presence of four of the major elements observed.

from 38° to 39° corresponding to (106) α SiC phase³². Consequently, the peak observed within the range from 44° to 45° corresponds to the peak of purified MWCNT (100)³³. The peak corresponding to 65° to 65° suggests the presence of α aluminium phase corresponding to planes (111)³⁴. The peak corresponding to the (420) plane of the CeO₂ element is also seen within the range from 78° to 79° ³⁵. XRD peaks observed within 82.35° to 82.40° diffraction angle refers to α Al₂O₃ at (111) diffraction phase³⁶. The presence of Al₂O₃ in the developed composite is due to the heating of parent material in the stir casting setup without an inert atmosphere. This confirms the presence of all the reinforcements incorporated into the matrix with relative homogeneity and is in close agreement with the EDS results.

Physical properties

The experimental and theoretical densities of the developed samples are presented pictorially in Fig. 9. The theoretical and experimental densities are very close to each other suggesting that the casting was good. Estimation of voids in the as-cast composite can be done by calculating the ratio given in equation 1 shown over the bar plot for each sample. This index remains well within 1.5% for all the samples measured. These deviations in theoretical and experimental densities may be attributed to minor casting defects or reinforcements drained away as slag among many other things. This further validates the emphasis on reinforcement preheating and mould preheating which are precautionary measures for reducing casting defects.

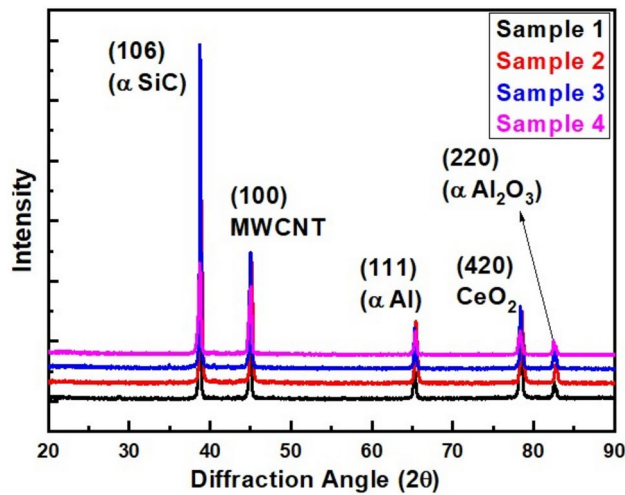


Fig. 8. XRD peaks of developed composites.

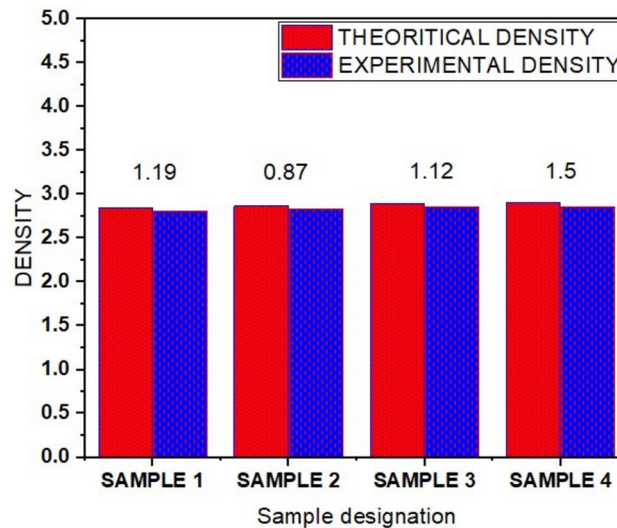


Fig. 9. Bar plot showing theoretical and experimental densities.

One of the major drawbacks of altering the chemical composition of an alloy to enhance its mechanical properties is the compromise that needs to be made with its physical properties like corrosion resistance. The development of composite materials involves very little to no alteration in the chemical composition of the material. Tafel plot is obtained by allowing electric current to flow through a finely polished and washed sample of the composite. Tafel plots of all the samples are shown in comparison with the base aluminium alloy in Fig. 10. The positive shift in corrosion potential with an increase in reinforcement percentage seen on the tafel plot suggests that the corrosion properties have improved with the addition of reinforcements. While it is not absolutely clear from the current study, the betterment in corrosion resistance may be attributed to one of the phases detected in the XRD analysis discussed in earlier sections. The incorporation of CeO₂ has been beneficial for corrosion properties in earlier works by Ashraf and Sibli^{37,38} and that is further validated by this study.

Mechanical properties

The hardness values of all four samples along with the comparison with as-cast base aluminium alloy (Al06063) are shown in Fig. 11. It can be seen from the bar graph that a significant increase in hardness values of aluminium composite is observed in comparison with the base material. Maximum average hardness of 93 HV was achieved at 2% CeO₂ after which the hardness saw a slight decline. The increase in hardness may have been due to good interfacial bonding between reinforcements and matrix materials. Past studies also suggest that the reinforcements are entrapped in inter-granular boundaries when the grain growth is dendritic which seems to be the case in the current work as seen from SEM images³⁹. The reinforcement particles entrapped around the grain boundary region hinders deformation leading to strengthening of the composite. The porosities index suggests that the maximum porosity was observed in the 4th sample. SEM images also reflect a slight agglomeration of

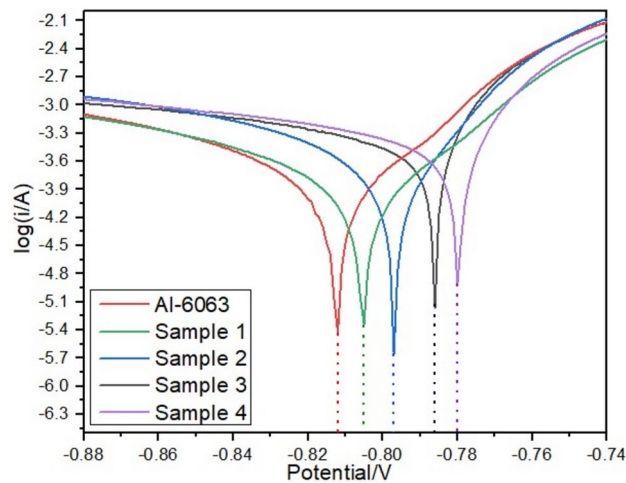


Fig. 10. Tafel Plot of composites with Al-6063.

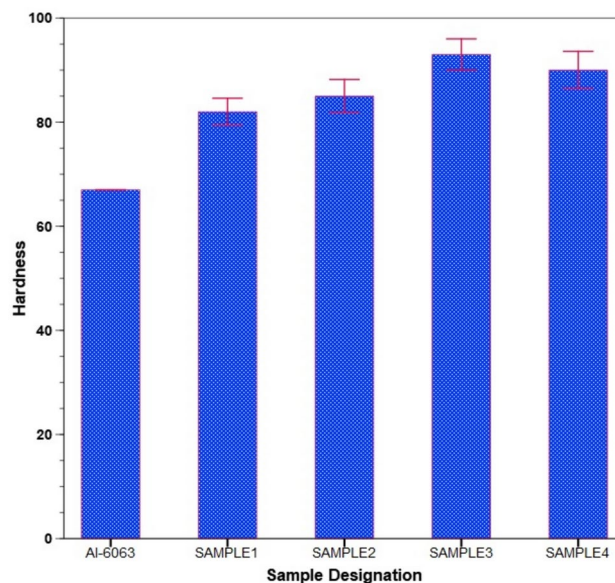


Fig. 11. Hardness comparison.

reinforcements in the fourth sample. These may be some of the reasons behind the slight decline in hardness values. It is also interesting to note that the hardness is at least 20% better than the base alloy which may be attributed to proper incorporation and homogeneous distribution of the reinforcements observed in SEM images.

The tensile test results were obtained as load-extension diagram for all the four samples which is shown in Fig. 12. This highlights the highest ultimate tensile stress as 165.62 MPa for the sample 3 which contained 2% CeO₂. Sample 1, sample 2 and sample 4 had the ultimate tensile strength of 153 MPa, 159 MPa and 162 MPa respectively. A comparison has also been made with the base aluminium alloy for all 4 samples in bar plot shown in Fig. 13. The tensile strength showed similar trends to hardness in terms of enhancement with respect to the CeO₂ percentage. It increased with an increase in reinforcement percentage up to 2% after which a slight downfall was observed. The maximum enhancement of 34% was achieved when CeO₂ was 2% of composite composition. The increase in tensile strength can be attributed to trapped reinforcement particles in inter-granular sites and good bond at the matrix reinforcement interfaces discussed in earlier sections. The downfall post optimum could be attributed to agglomeration and casting defects which were most prominent in the sample with 2.5% CeO₂. The unreinforced aluminium alloy failed at ultimate tensile strength at 123 MPa with a cup and cone fracture while the mode of fracture seemed more brittle (very little permanent deformation) as the reinforcement percentage increased. The least permanent deformation was exhibited by sample 4 along with the downfall in tensile strength upon increasing the reinforcement percentage.

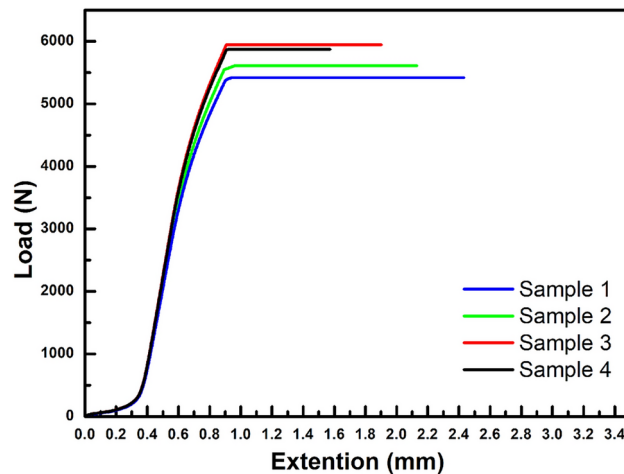


Fig. 12. Load-extension plot for the fabricated composites.

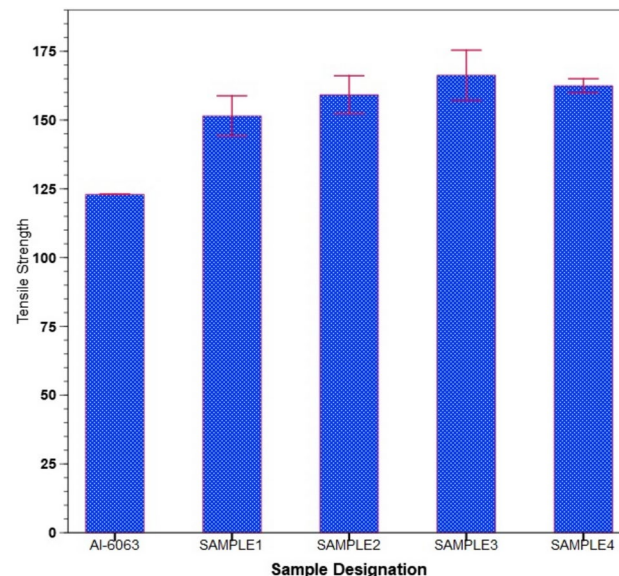


Fig. 13. Tensile strength comparison.

Conclusion

Four samples of rare earth element-reinforced hybrid aluminium composites were developed using a conventional stir-casting process to study morphological, mechanical and physical properties. Four samples were varied for their CeO₂ composition from 1% to 2.5% while keeping the weight percentages of SiC and MWCNT constant at 1% and 0.1%. Following conclusions can be made from the current work

- Preheating of reinforcement at 280°C, thorough stirring of reinforcements at 400 RPM for 7 minutes and proper preheating of mold resulted in a homogeneous reinforcement distribution as confirmed by the SEM images and colour maps.
- XRD analysis showed the presence of all the reinforcements incorporated into the matrix which was also confirmed using EDS analysis.
- Very little porosity was estimated based on a comparison between theoretical and experimental densities suggesting proper casting. Preheating of mold helped in ensuring good casting.
- Corrosion properties were slightly better for all composites. An increase in CeO₂ percentage resulted in the betterment of corrosion potential with the best corrosion potential showed by the sample containing 2.5% CeO₂.
- The developed composite showed enhanced hardness with the maximum hardness of 93 HV shown by the 3rd sample. The poor hardness of the 4th sample may be attributed to agglomeration of reinforcement which is visible in SEM images of this sample. Tensile results showed similar trends to that of hardness which in-

creased up to 2% CeO₂ having the ultimate tensile strength of 166.3 MPa followed by a decline in ultimate tensile strength.

Data availability

The data presented in this study are available through email upon request to the corresponding author.

Received: 23 April 2024; Accepted: 4 November 2024

Published online: 13 November 2024

References

- Kelly, A. Composite materials after seventy years. *J. Mater. Sci.* **41**(3), 905–912. <https://doi.org/10.1007/s10853-006-6569-9> (2006).
- Janszen, F. H. A. & Vloemans, M. P. F. Innovation and the materials revolution. *Technovation* **17**(10), 549–594. [https://doi.org/10.1016/S0166-4972\(97\)00041-2](https://doi.org/10.1016/S0166-4972(97)00041-2) (1997).
- Varvani-Farahani, A. Composite materials: Characterization, fabrication and application-research challenges and directions. *Appl. Compos. Mater.* **17**(2), 63–67. <https://doi.org/10.1007/s10443-009-9107-5> (2010).
- Surappa, M. K. Aluminium matrix composites: Challenges and opportunities. *Sadhana* **28**(1–2), 319–334. <https://doi.org/10.1007/BF02717141> (2003).
- Pastuszak, P. D. & Muc, A. Application of composite materials in modern constructions. *Key Eng. Mater.* **542**, 119–129. <https://doi.org/10.4028/www.scientific.net/KEM.542.119> (2013).
- Chakrapani, P. & Suryakumari, T. S. A. Mechanical properties of aluminium metal matrix composites-A review. *Mater. Today* **45**, 5960–5964. <https://doi.org/10.1016/j.matpr.2020.09.247> (2021).
- Bhong, M. et al. Review of composite materials and applications. *Mater. Today*[SPACE]<https://doi.org/10.1016/j.matpr.2023.10.026> (2023).
- Orhadahwe, T. A., Ajide, O. O., Adeleke, A. A. & Ikubanni, P. P. A review on primary synthesis and secondary treatment of aluminium matrix composites. *Arab J. Basic Appl. Sci.* **27**(1), 389–405. <https://doi.org/10.1080/25765299.2020.1830529> (2020).
- Li, M., Guo, Q., Chen, L., Li, L., Hou, H., & Zhao, Y. **21** 4138–4150 ISSN 2214-7853 <https://doi.org/10.1016/j.jmrt.2022.11.067>
- Khalid, M. Y., Umer, R. & Khan, K. A. Review of recent trends and developments in aluminium 7075 alloy and its metal matrix composites (MMCs) for aircraft applications. *Results Eng.* **20**, 101372. <https://doi.org/10.1016/j.rineng.2023.101372> (2023).
- Chandel, R., Sharma, N. & Bansal, S. A. A review on recent developments of aluminum-based hybrid composites for automotive applications. *Emerg. Mater.* **4**(5), 1243–1257. <https://doi.org/10.1007/s42247-021-00186-6> (2021).
- Shao, L., Xue, N., Li, W., Liu, S., Tu, Z., Chen, Y., Zhang, J., Dai, S., Liu, Q., Shi, X., Wang, T., Chen, M., Huang, Y., Xu, F., & Zhu, L. **11** 959 ISSN 2227-9717 <https://doi.org/10.3390/pr11030959>
- Liu, W., Yue, X., Hu, Q., Song, Y., Zhu, B., Chen, X., & Huang, H. **985** 174045 ISSN 0925-8388 <https://doi.org/10.1016/j.jallcom.2023.174045><https://doi.org/10.1016/j.scriptamat.2023.115763><https://doi.org/10.1016/j.msea.2023.144965><https://doi.org/10.3390/ma16144725>
- Suresh, S., Natarajan, E., Mohan, D. G., Ang, C. K. & Sudhagar, S. Depriving friction stir weld defects in dissimilar aluminum lap joints. *Proc. Inst. Mech. Eng. Part E*[SPACE]<https://doi.org/10.1177/09544089241239817> (2024).
- Prakash, S., Sasikumar, R., Natarajan, E. & Suresha, B. Influence of feeding techniques in bottom tapping stir casting process for fabrication of alumina nano-filler-reinforced aluminium composites. *Trans. Indian Inst. Metals* **73**(5), 1265–1272. <https://doi.org/10.1007/s12666-020-01975-z> (2020).
- Purohit, R., Qureshi, M. M. U. & Jain, A. Forming behaviour of aluminium matrix nano Al₂O₃ composites for automotive applications. *Adv. Mater. Process. Technol.* **6**(2), 272–283. <https://doi.org/10.1080/2374068X.2020.1731665> (2020).
- Khan, M. et al. Study of microstructure and mechanical behaviour of aluminium alloy hybrid composite with boron carbide and graphene nanoplatelets. *Mater. Chem. Phys.* **271**, 124936. <https://doi.org/10.1016/j.matchemphys.2021.124936> (2021).
- Peter, P. & Adekunle, A. A. A review of ceramic/bio-based hybrid reinforced aluminium matrix composites. *Cogent Eng.* **7**(1), 1727167. <https://doi.org/10.1080/23311916.2020.1727167> (2020).
- Raailay, A., Chatterjee, S., Ghadai, R. K., Das, P. P. & Chakraborty, S. Optimization of hybrid Al-MMC drilling using a new RAMS-RATMI-based approach. *Int. J. Interact. Des. Manuf.*[SPACE]<https://doi.org/10.1007/s12008-023-01628-7> (2023).
- Bhowmik, A., Dey, D. & Biswas, A. Comparative study of microstructure, physical and mechanical characterization of SiC/TiB₂ reinforced aluminium matrix composite. *Silicon* **13**(6), 2003–2010. <https://doi.org/10.1007/s12633-020-00591-2> (2021).
- Zhang, C., Khorshidi, H., Najafi, E., & Ghasemi, M. **384** 135390 ISSN 0959-6526 <https://doi.org/10.1016/j.jclepro.2022.135390><https://doi.org/10.1007/s11663-023-02994-y>
- Pazhani, A. et al. Synthesis and characterisation of graphene-reinforced AA 2014 MMC using squeeze casting method for lightweight aerospace structural applications. *Mater. Des.* **230**, 111990. <https://doi.org/10.1016/j.matdes.2023.111990> (2023).
- Akinwande, A. A. et al. Tribological performance of a novel 7068-aluminium/lightweight-high-entropy-alloy fabricated via powder metallurgy. *Mater. Chem. Phys.* **308**, 128207. <https://doi.org/10.1016/j.matchemphys.2023.128207> (2023).
- Ananiadis, E. A., Karantzalis, A. E., Sfikas, A. K., Georgatis, E. & Matikas, T. E. Aluminium matrix composites reinforced with AlCrFeMnNi HEA Particulates: Microstructure. *Mech. Corros. Prop. Mater.* **16**(15), 5491. <https://doi.org/10.3390/ma16155491> (2023).
- Cheneke, S. & Karunakar, D. B. Development of AA2024/TiB₂+Y₂O₃ hybrid composites with improved mechanical properties through stir rheocasting. *Arab. J. Sci. Eng.* **45**, 1155–1171 (2020).
- Kumar, D., Angra, S. & Singh, S. Synthesis and characterization of DOE-based stir-cast hybrid aluminum composite reinforced with graphene nanoplatelets and cerium oxide. *Aircraft Eng. Aerosp. Technol.* **95**(10), 1604–1613. <https://doi.org/10.1108/AEAT-04-2023-0104> (2023).
- Kumar, N., Navin, K., Ball, R. J. & Kurchania, R. Mechanical and structural properties of aluminium nanocomposites reinforced with cerium oxide nanoparticles fabricated by powder metallurgy. *J. Mater. NanoSci.* **7**(2), 2 (2020).
- Suresh, S., Natarajan, E., Mohan, D. G., Ang, C. K. & Sudhagar, S. Depriving friction stir weld defects in dissimilar aluminum lap joints. *Inst. Mech. Eng.*[SPACE]<https://doi.org/10.1177/09544089241239817> (2024).
- Suresh, S., Natarajan, E., Franz, G. & Rajesh, S. Differentiation in the SiC filler size effect in the mechanical and tribological properties of friction-spot-welded AA5083-H116 alloy. *Fibers*. <https://doi.org/10.3390/fib10120109> (2022).
- Suresh, S. et al. Performance Analysis of nano silicon carbide reinforced swept friction stir spot weld joint in AA6061-T6 alloy. *Silicon* **13**, 3399–3412. <https://doi.org/10.1007/s12633-020-00751-4> (2020).
- Suresh, S. et al. Effect of the overlap ratio on surface properties of 7B04 aluminum alloy for aviation during laser derusting. *J. Mater. Res. Technol.* <https://doi.org/10.1016/j.jmrt.2022.07.129> (2022).
- Izhevskiy, V. A., Genova, L. A., Bressiani, A. H. A., & Bressiani, J. C. Liquid phase sintered SiC. Processing and transformation controlled microstructure tailoring. *Mater. Res.*, **3**(4), 131–138. <https://doi.org/10.1590/S1516-1439200000400007> (2000).
- Atchudan, R., Pandurangan, A. & Joo, J. Effects of nanofillers on the thermo-mechanical properties and chemical resistivity of epoxy nanocomposites. *J. Nanosci. Nanotechnol.* **15**(6), 4255–4267. <https://doi.org/10.1166/jnn.2015.9706> (2015).

34. Ali, L. F., Kuppuswamy, N., Soundararajan, R., Ramkumar, K. R. & Sivasankaran, S. Microstructural evolutions and mechanical properties enhancement of AA 6063 alloy reinforced with Tungsten (W) nanoparticles processed by friction stir processing. *Mater. Charact.* **172**, 110903. <https://doi.org/10.1016/j.matchar.2021.110903> (2021).
35. Wang, G., Mu, Q., Chen, T. & Wang, Y. Synthesis, characterization and photoluminescence of CeO₂ nanoparticles by a facile method at room temperature. *J. Alloys Compd.* **493**(1–2), 202–207. <https://doi.org/10.1016/j.jallcom.2009.12.053> (2010).
36. Li, Z., Wu, K., Cao, J., & Wang, Y. Controlled synthesis of γ -Al₂O₃ via the hydrothermal-pyrolysis method. In *IOP Conference Series: Materials Science and Engineering* Vol. 207, No. 1, 012004 (IOP Publishing, 2017).
37. Ashraf, P. M. & Shibli, S. M. A. Reinforcing aluminium with cerium oxide: A new and effective technique to prevent corrosion in marine environments. *Electrochem. Commun.* **9**(3), 443–448. <https://doi.org/10.1016/j.elecom.2006.09.010> (2007).
38. Ashraf, P. M. & Shibli, S. M. A. Development of CeO₂- and TiO₂-incorporated aluminium metal-composite matrix with high resistance to corrosion and biofouling. *J. Solid State Electrochem.* **12**(3), 315–322. <https://doi.org/10.1007/s10008-007-0393-2> (2008).
39. Kim, G.-H. et al. Effect of oxide dispersion on dendritic grain growth characteristics of cast aluminum alloy. *Mater. Trans.* **51**(10), 1951–1957. <https://doi.org/10.2320/matertrans.M2010166> (2010).

Acknowledgements

This article was co-funded by the European Union under the REFRESH – Research Excellence For REgion Sustainability and High-tech Industries project number CZ.10.03.01/00/22_003/0000048 via the Operational Programme Just Transition and has been done in connection with project Students Grant Competition SP2024/087 „Specific Research of Sustainable Manufacturing Technologies“ financed by the Ministry of Education, Youth and Sports and Faculty of Mechanical Engineering VSB-TUO.

Author contributions

Conceptualization, Formal analysis, Investigation, Methodology, Writing - original draft, Writing - review & editing: Gaurav Sapkota, Ranjan Kumar Ghadai, Soham Das, Asish Sharma, Robert Cep, Kanak Kalita; All authors reviewed the manuscript.

Funding

This article was supported by the project SP2024/087 from Ministry of Education Youth and Sport of Czech Republic and VSB-TUO.

Declarations

Competing interests

The authors declare no competing interests.

Additional information

Correspondence and requests for materials should be addressed to R.K.G. or K.K.

Reprints and permissions information is available at www.nature.com/reprints.

Publisher's note Springer Nature remains neutral with regard to jurisdictional claims in published maps and institutional affiliations.

Open Access This article is licensed under a Creative Commons Attribution-NonCommercial-NoDerivatives 4.0 International License, which permits any non-commercial use, sharing, distribution and reproduction in any medium or format, as long as you give appropriate credit to the original author(s) and the source, provide a link to the Creative Commons licence, and indicate if you modified the licensed material. You do not have permission under this licence to share adapted material derived from this article or parts of it. The images or other third party material in this article are included in the article's Creative Commons licence, unless indicated otherwise in a credit line to the material. If material is not included in the article's Creative Commons licence and your intended use is not permitted by statutory regulation or exceeds the permitted use, you will need to obtain permission directly from the copyright holder. To view a copy of this licence, visit <http://creativecommons.org/licenses/by-nc-nd/4.0/>.

© The Author(s) 2024